Vulliet, L.; Laloui, L.; Koliji, A.; Cuisinier, O.

Unsaturated structured soil with multi-porosity (Multi-poröse Strukturen in teilgesättigten Böden)

Verfügbar unter/Available at: https://hdl.handle.net/20.500.11970/102169

Vorgeschlagene Zitierweise/Suggested citation:
Vulliet, L.; Laloui, L.; Koliji, A.; Cuisinier, O. (2004): Unsaturated structured soil with multi-porosity (Multi-poröse Strukturen in teilgesättigten Böden). In: Bundesanstalt für Wasserbau (Hg.): Boden- und Sohl-Stabilität - Betrachtungen an der Schnittstelle zwischen Geotechnik und Wasserbau
Soil and Bed Stability - Interaction Effects between Geotechnics and Hydraulic Engineering. Karlsruhe: Bundesanstalt für Wasserbau.

4 Unsaturated structured soil with multi-porosity

Multi-poröse Strukturen in teilgesättigten Böden

L. Vulliet, L. Laloui, A. Koliji & O. Cuisinier

Swiss Federal Institute of Technology Lausanne, Switzerland (EPFL)
Eidgenossische Technische Hochschule Lausanne, Schweiz (EPFL)

ABSTRACT: Soil structure properties are of great importance in a variety of engineering applications. The behavior of such soil is however rather complex and very few results are available to model their hydro-mechanical properties. Some recent laboratory results are presented in this paper. They concern the hydro-mechanical response of soil consisting of unsaturated aggregate assemblies. A new oedometer cell for testing unsaturated soil samples under mechanical (external axial load) and hydric stress (matric suction) is used. Stress-strain behavior under various suction levels is discussed. The main results focus on the pore-size distribution of a natural soil with multi-porosity and its variation with total stress and suction. Mercury intrusion porosimetry (MIP) is used here. It is shown how the volume fraction of macropores and micropores decreases, respectively increases, when suction increases.

KURZFASSUNG: Die Eigenschaften von multi-porösen Strukturen in Böden sind im Ingenieurwesen von großer Bedeutung. Das Verhalten solcher Böden ist jedoch sehr komplex. Zudem liegen nur sehr wenige Versuchsergebnisse zur Modellierung der hydro-mechanischen Eigenschaften vor. Der vorliegende Artikel stellt einige neue Ergebnisse von Laborversuchen vor. Sie betreffen die hydro-mechanische Reaktion von teilgesättigten, aus unterschiedlichen Strukturaggregaten zusammengesetzten Böden. Für die Untersuchung von teilgesättigten Bodenproben unter mechanischer (äußere axiale Last) und hydraulischer (Matrix-Saugspannung) Last wird eine neue Ödometerzelle benutzt. Das Spannungs-Dehnungsverhalten wird für verschiedene Saugspannungen untersucht. Die Hauptergebnisse konzentrieren sich auf die Porengrößenverteilung eines natürlichen multi-porösen Bodens und deren Änderung mit der Gesamt- und der Saugspannung. Hierzu wird die „Mercury intrusion porosimetry (MIP)” Technik verwendet. Es wird gezeigt, wie sich die Volumenverteilung von Makro- und Mikroporen mit dem Anstieg der Saugspannung verändert.

4.1 Introduction

Soil structure properties are of great importance in a variety of engineering applications, mainly geotechnical (e.g. behavior of fissured soils), geo-environmental (e.g. clay pallets for radioactive waste barrier) and agricultural engineering (e.g. soil compaction due to heavy machineries).

Natural soils show different structures, characterized by structural units, such as aggregates, porous block, fissures, even earth worm holes and root channels. As a simplification, they can be categorized in two groups (Figure 4.1): aggregate assemblies and fissured porous media. The geometrical description of such structure (the soil fabric) is not an easy task, since the geometry of pores is much more complex than the geometry of grain, commonly used in grain-size distribution analysis. In this study, we will restrict ourselves to a simple scalar function: the pore-size distribution (PSD), neglecting other important factors such as pore orientation, pore connectivity, tortuosity, etc.

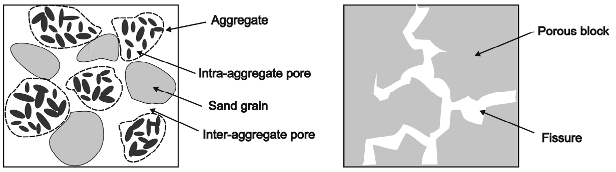

Figure 4.1 Structured soils: aggregate assembly (left) and fissured porous medium (right)

In both cases, the presence of a *micro*porosity inside the (deformable) aggregates or blocks and a *macro*-porosity at a larger inter-aggregate scale strongly influence the hydro-mechanical behavior: compressibility /Lambe 1958/, hydraulic conductivity /Tamari 1984/ soil-water characteristic curve /Brustaert 1968/, solute transport /Koch & Flühler 1993/, etc.

Such a division of pores into macro and micro levels leads to the concept of double porosity for soils. It has been used by many authors, both for testing and modeling, e.g. /Delage & Lefebvre 1984/, /Coulon & Bruand 1989/, /Lapierre et al. 1990/, /Griffiths & Joshi 1990/, /Valliappan & Khalili 1990/, /Gens et al. 1995/, /Tuncay & Corapcioglu 1995/, /Al-Mukhtar et al. 1995, 1996/, /Delage et al. 1996/, /Wang & Berryman 1996/, /Simms & Yanful 2001, 2002/, /Cuisinier & Laloui 2004/.

In such systems, although most of the fluid mass is stored in the micropores, the permeability of the macropores is much higher than that of the micropores. This leads to a dually permeable medium and also to two distinct fluid pressure fields: one in the macropores and the other in the micropores. Therefore, the fluid pressures contained in the two types of pores may reach equilibrium at different rates, and virtually independently, if the channels for fluid transport between the two types of pores are restricted.

Deformation of an aggregated soil under stress (external load or internal fluid phase pressure) is the result of aggregate rearrangements (as in conventional soil mechanics) and aggregate inner strains. This rather complex behavior is not yet fully understood and properly modeled, in particular in the case of unsaturated soils.

The purpose of this paper is to present some very recent research results obtained at the Soil Mechanics Laboratory of EPFL, in collaboration with other advanced research teams.

4.2 Tested Soils and Sample Preparation

The tested soil is a sandy loam (morainic soil) coming from the eastern part of Switzerland. The average plasticity index of the soil is I_P = 12 % and the liquid limit w_L = 30 %. All the samples used in this study were prepared using the same procedure. After sampling in the field, the soil was air-dried; after several days it was gently crushed and aggregates between 0.4 and 2 mm were selected by sieving (see Figure 4.2). They were then wetted up to a mass water content of about w = 15 % and stored in an airtight container for at least one week in order to reach moisture equilibrium. The material was then statically compacted directly inside the testing device (a new oedometer cell, see below) up to a dry density of 14 kN.m^{-3}. In a last stage the samples were saturated.

Figure 4.2 Picture of the tested soil (max grain size approx. 2 mm)

4.3 Mercury Intrusion Porosimetry

Several techniques can be applied to determine the pore-size distribution. Here, the mercury intrusion porosimetry (MIP) is used (see e.g. /Penumadu & Dean 2000/). The theoretical bases for the determination of soil fabric with MIP are very similar to those of the pressure plate test. In the case of MIP, the non-wetting fluid is mercury and air is the wetting fluid. The mercury pressure is increased by steps and the intruded volume of mercury is monitored for each pressure increment. Assuming that soil pores are cylindrical flow channels, Jurin's equation can be used to determine the pore radius $R(\psi)$ associated with each mercury pressure, ψ :

$$\psi = \frac{2\,T_s}{R(\psi)} \qquad (4\text{-}1)$$

where T_s is the surface tension of the mercury.

Due to technical requirements, tested samples must be totally dry in order to perform a MIP test. Among the available dehydrating methods, oven drying and air-drying should be avoided since they induce strong soil pore geometry modification. According to /Delage & Lefebvre 1984/, the freeze-drying method is the least disturbing preparation technique for water removal. Hence, this method was selected for our study. For more details see /Cuisinier & Laloui 2003/.

A MIP test gives the cumulative mercury volume intruded as a function of the pore radius. To further interpret MIP data, /Juang & Holtz 1986/ have proposed using the pore size distribution, PSD, of the sample, defined as follows:

$$f(\log r_i) = \frac{\Delta V_i}{\Delta(\log r)} \qquad (4\text{-}2)$$

where ΔV_i is the injected mercury volume at a given pressure increment corresponding to pores having a radius of $r_i \pm (\Delta \log r_i)/2$. It is necessary to use a logarithmic scale because wide ranges of pore radius, meaning several orders of magnitude, are investigated.

4.4 Hydro-mechanical loading

4.4.1 A new oedometer cell

A new suction-controlled oedometer has been developed at LMS-EPFL (Figure 4.3). This device uses the air overpressure method for suction control. The ceramic disc at the base of the sample has an air entry value of 500 kPa. An air pressure/volume controller regulates the air pressure inside the sample, u_a, while the water pressure at the base of the sample, u_w, is maintained constant with a water pressure/volume controller. The imposed matric suction is $s = u_a - u_w$. The vertical mechanical stress, σ_v, (maximum 1 MPa) is transmitted to the soil sample through the upper chamber of the device, a water tank made with a flexible membrane. The sample diameter is 63.5 mm and the initial height about 12 mm.

With such a device, the effect of mechanical loading (i.e. change of σ_v), hydric loading (i.e. change of s) and combination of both can be investigated. Global sample strain is determined from (vertical) displacement measurements, water content by extracted water volume measurement and pore-size distribution by MIP after removal of the sample.

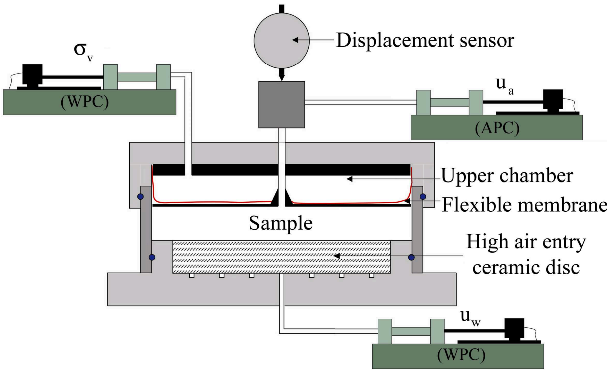

Figure 4.3 *Suction-controlled oedometer (APC: air pressure controller; WPC: water pressure controller). /Cuisinier & Laloui 2003/*

4.4.2 Effect of mechanical loading

Figure 4.4 shows the effect of total vertical stress σ_v on the global sample void ratio, e, for two different samples (i.e. saturated condition, s = 0, and unsaturated condition, s = 200 kPa).

The preconsolidation pressure of the unsaturated sample is significantly higher than the one of the saturated sample. This observation is confirmed by several authors (e.g. /Alonso et al. 1990/). The values of the compressibility indices C_c and C_s are also higher in the case of the unsaturated sample, for this specific value of suction. /Geiser 1999/ made similar observations on a silt and correlated the air entry value of the material with the suction for which C_c is maximal. /Sivakumar & Wheeler 2000/

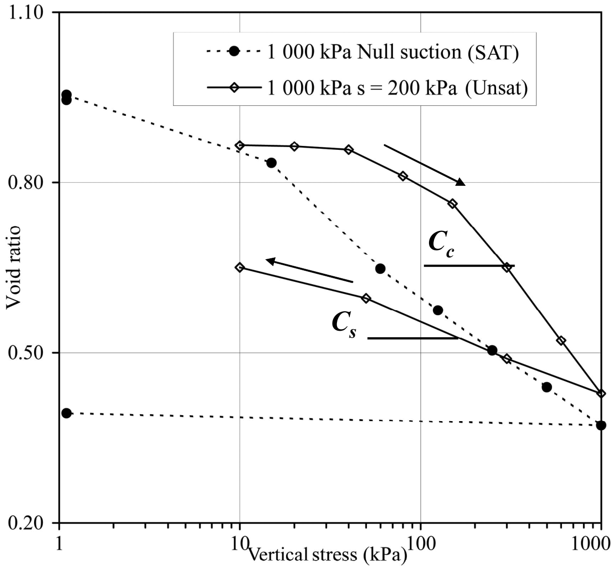

Figure 4.4 *Comparison of the compression curves under s = 0 (null suction, saturated case) and s = 200 kPa. /Cuisinier & Laloui 2003/.*

obtained similar behavior for lightly compacted kaolin. They demonstrated that this mechanical behaviour depends on the initial density of the material. The material behavior observed in the tests presented in this paper is certainly related to the relatively loose initial density of the samples related to their low density. This is supported by data obtained by /Cuisinier 2002/ on a compacted swelling soil.

Recent results (not shown here) demonstrate as expected that the compressibility of structured soil (assembly of aggregates) is larger than the compressibility of the matrix of the single aggregate.

Figure 4.5 shows the effect of a change in (total) vertical stress σ_v on the pore-size distribution (PSD) of the saturated aggregated soil. PSD are determined for stresses of σ_v = 15, 60, 250, and 1000 kPa.

It can be seen that the effect of stress increase mainly results in reducing the size of macropores, while micropores are only slightly affected.

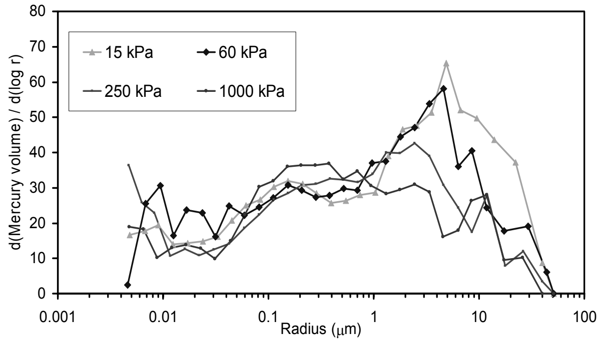

Figure 4.5 *Effect of applied vertical stress to the pore-size distribution /Cuisinier & Laloui, 2004/*

4.4.3 Effect of suction on pore-size distribution

Figure 4.6 shows the effect of suction s on the pore-size distribution of the structured soil material. Here, the effect is more pronounced than in the case of mechanical loading. From Figure 4.6 (and 4.7), four different zones of pore classes can be recognized: Zones 1 and 4 are related to the pores which are only slightly affected by suction and on which the influence of suction can be neglected. Zone 2 corresponds to the micropores; the volume fraction of these pores increases as suction increases. The pore volume fraction of the pores in Zone 3 reduces as suction increases. The behavior of these pore classes are different and they will be distinguished in the model formulation. Three pore radii R_1, R_2 and R_3 determine the limits between pore zones.

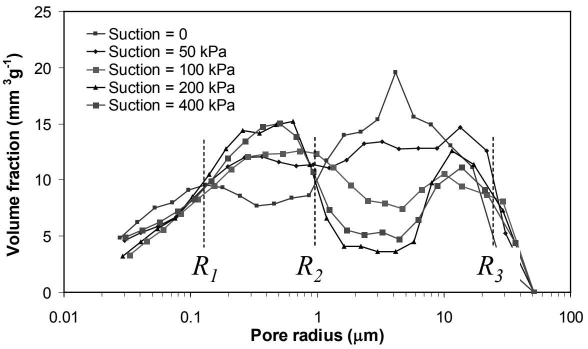

Figure 4.6 *Effect of applied suction to the pore-size distribution (adapted from /Cuisinier & Laloui 2004/)*

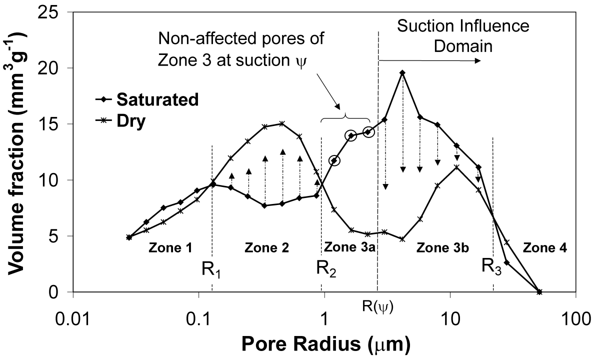

Figure 4.7 *Suction influence domain and evolution of pore classes /Koliji et al. 2004/*

4.5 Modeling pore-size changes

4.5.1 Description

A mathematical model has been developed to predict the change in pore-size distribution induced by suction changes /Koliji et al. 2004/. The modeling concept is as follows: given two limit cases, the saturated case (zero suction, or initial case) and the driest case (suction of 400 kPa, or final case in this specific study), predict the modification of the PSD curves for intermediate cases.

The suction influence domain (Figure 4.7) is defined, for a specific suction ψ, as the pore radii potentially drained according to Equation 4-1. Details can be found in /Koliji et al. 2004/. The final model reads:

$$
\begin{array}{ll}
v(r,\psi) = v(r,\psi_0) & ;\ r < R_1 \\
v(r,\psi) = v(r,\psi_0) + C_2 \cdot (v(r,\psi_f) - v(r,\psi_0)) & ;\ R_1 < r < R_2 \\
v(r,\psi) = v(r,\psi_0) & ;\ R_2 < r < R(\psi) \\
v(r,\psi) = v(r,\psi_0) - C_3 \cdot (v(r,\psi_0) - v(r,\psi_f)) & ;\ R(\psi) < r < R_3 \\
v(r,\psi) = v(r,\psi_0) & ;\ r > R_3
\end{array}
\qquad (4\text{-}3)
$$

where $v(r,\psi)$ is the pore-size volume fraction at suction ψ (or s), ψ_o the initial suction,

ψ_f the final suction, and C_3 and C_3 material constants defined as:

$$V_\psi = \sum_{r>R(\psi)} (v(r,\psi_o) - v(r,\psi_f)) \quad ; \quad (R_2 < r, R(\psi) < R_3)$$

$$V_3 = \sum_{R_2<r<R_3} (v(r,\psi_0) - v(r,\psi_f)) \qquad C_3 = \left(\frac{V_\psi}{V_3}\right)^2$$

$$V_2 = \sum_{R_1<r<R_2} (v(r,\psi_f) - v(r,\psi_0)) \qquad C_2 = \frac{V_2}{V_3}$$

(4-4)

4.5.2 Validation

The initial data needed for the model are the PSD curves for the saturated (s = 0 kPa) and driest (s = 400 kPa) states. The model predictions made for the PSD curves at suction levels of 50, 100 and 200 kPa have been analyzed.

Figure 4.8 shows the comparison of the modeled and measured PSD curves at a suction of 200 kPa. The agreement is quite satisfactory.

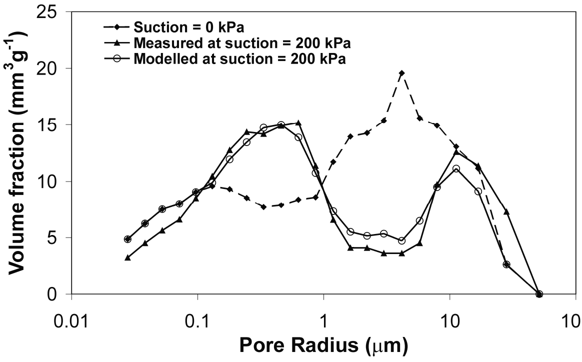

Figure 4.8 Modeled and measured PSD at suction of 200 kPa /Koliji et al. 2004/

4.6 Neutron Beam Testing

In the ongoing Swiss joint research testing program between LMS-EPFL (soil mechanics), ITÖ-ETHZ (soil physics), and PSI (Paul Scherer Institute, Villigen) the neutron beam line (NEUTRA) is used to perform 2D and 3D testing of unsaturated structured soils. This experiment in itself is, to our knowledge, a world premiere.

Tomography is a method which provides cross-sectional images of an object from transmission data, measured by irradiating it from many different directions (http://neutra.web.psi.ch/What/tomo.html, Figure 4-9). The non-destructive analysis of an object by neutron radiography is mostly done taking one or more 2D parallel projections by rotating the object in small angular steps over 180° and calculating tomographic slices using the inverse Radon transform.

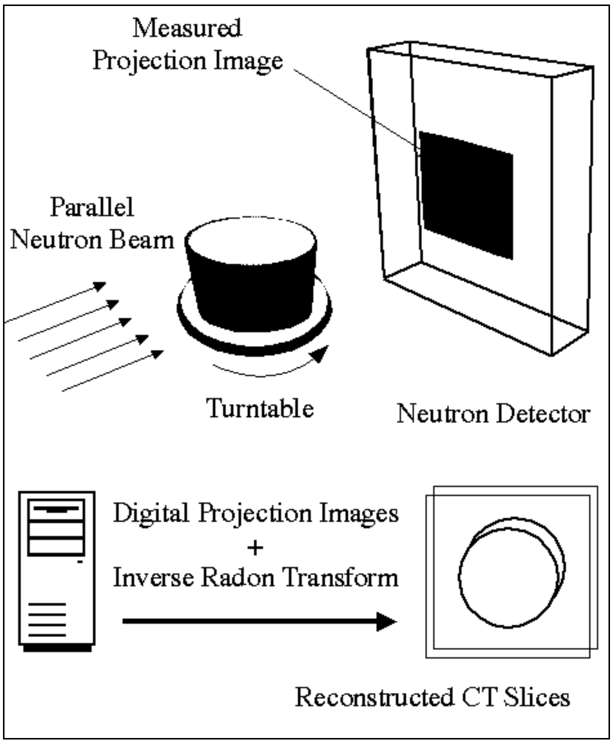

Figure 4.9 Schematics of Neutron Tomography (Paul Scherer Institute, Switzerland - http://neutra.web.psi.ch/What/tomo.html)

Recent studies performed by ITÖ-ETHZ show the successful use of neutron radiography (transmission) and tomography to monitor the movement of water (H_2O) in structured media saturated with deuterium water (D_2O).

For assessing the water exchange between aggregates (with the interaggregate pore space being drained) some aggregates are desaturated with D_2O (transparent in the neutron beam) at a given suction and some with H_2O (strongly neutron absorbing) at a different suction value. Water exchange is then monitored in real time using 2D scans. The final configuration, the resulting deformation of the aggregates and the spatial configuration of the macropore space are also observable in the neutron radiographs (see Figure 4.10).

The objective of this ongoing project is to improve the understanding of the effect of structure on the mechanical properties and fluid flows of soils under non-saturated conditions. It also link research of two related fields (Soil Mechanics and Soil Physics) that developed similar concepts over the past decades with a very different focus and under differing conditions and assumptions.

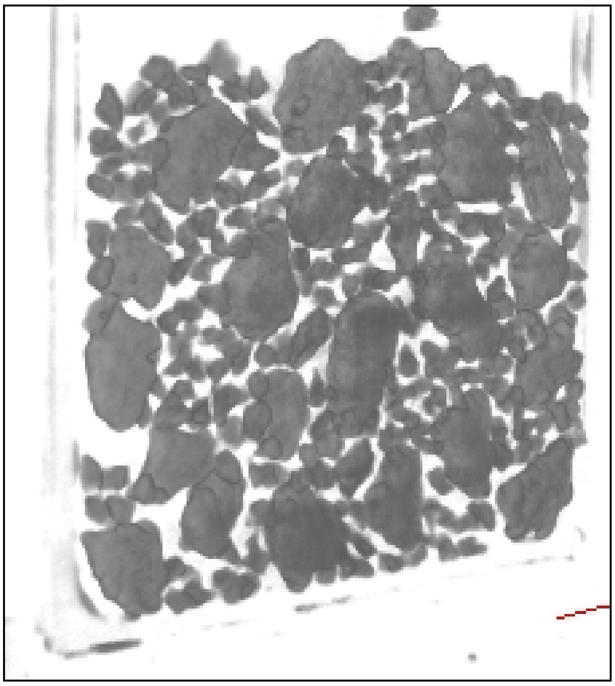

Figure 4.10 Image of a structured soil from Neutron Beam Testing 50x50x8 mm /Carminati, 2004/

4.7 Conclusion

This paper presents several results of a study undertaken to characterize the hydromechanical behavior and the fabric evolution imposed by stress/suction loading of a compacted soil.

A new suction-controlled oedometer using the air overpressure method is presented. The pore space geometry of the soil was determined with mercury injection porosimetry (MIP). The data confirm that suction has a strong influence on the deformation process of soil. It shows that, for the same applied mechanical stress, fabric is strengthened by suction. In addition, the volume fraction of micropores is higher in the unsaturated sample than in the saturated one. Finally, not all macropores disappear when applying even large values of stress/suction.

An interpolation model is presented for the numerical simulation of the modification of the pore space geometry of the structured double porosity soil subjected to suction increase. This model is mainly based on the concept of the suction influence domain. The model divides the pore size domain into different zones: macropores, micropores and domains where the suction effect is limited. Each zone has its own behavior and the micropore and the macropore zones are strongly coupled. The numerical simulations show that the model is able to reproduce the main aspects of suction-induced effects on soil structure.

The neutron tomography technique is used to perform 2D and 3D testing of unsaturated structured soils. This experiment is done jointly between our lab and ITÖ-ETHZ and PSI. Water exchange between aggregates, using deuterium D_2O and water H_2O at different suction value, is monitored in real time using 2D scans. The resulting deformation of the aggregates and the spatial configuration of the macropore space are observable in the neutron radiographs.

These various investigations should improve the understanding of the effect of structure on the mechanical properties and fluid flows of structured soils under non-saturated conditions.

4.8 Acknowledgements

The authors thank Dr Peter Weisskopf and Dr Th. Anken for providing the soil used and the assistance of the Powder Technology Laboratory (EPFL) to perform the freeze-dryings. This research was funded by the Swiss Agency for Environment, Forests and Landscape (contract n° 2001.H.10 granted to the second author), and by the ETH Board. Thanks to our partners at ITÖ-ETHZ, Prof. H. Fluehler and Mr A. Carminati, and at PSI for the access to the neutron beam facility, and in particular Dr E. Lehmann and Mr P. Vöntobel.

4.9 References

Al-Mukhtar, M. 1995

Macroscopic behavior and microstructural properties of a kaolinite clay under controlled me-chanical and hydraulic state. In Alonso, E.E. & Delage, P. (eds.), Unsaturated Soils: Proc. 1st Int. Conf. on Unsaturated Soils / UNSAT 95: 3-9. Paris, 6-8 Septembre 1995.

Al-Mukhtar, M., Belanteur, N., Tessier, D. & Vanapalli, S.K. 1996

The fabric of a clay soil under controlled mechanical and hydraulic stress states. Applied Clay Science 11: 99-115

Alonso, E.E., Gens, A. and Josa, A., 1990

A constitutive model for partially saturated soils. Géotechnique, 40, pp. 405-430.

Brustaert, W. 1968

The permeability of a porous medium de-termined from certain probability laws for pore-size distribution. Water Resources Research 4: pp. 425-434

Carminati, A. 2004

Image from Neutron Beam Testing at PSI, Preliminary tests, Personnal communication, 2004

Coulon, E. & Bruand, A. 1989

Effects of compaction on the pore space geometry in sandy soils. Soil and Tillage Research 15: pp. 137-152

Cuisinier, O. 2002

Hydromechanical behaviour of compacted swelling soils (in french). PhD thesis, INPL, Nancy, France, 165 p.

Cuisinier, O. & Laloui, L. 2003

Fabric Evolution of an Unsaturated Compacted Soil during Hydromechanical Loading, International Confenrence “From Experimental Evidence Towards Numerical Modelling of Unsaturated Soils”, Weimar. Springer Proceedings in Physics, Vol. 93, pp. 147-158.

Cuisinier, O. & Laloui, L. 2004

Fabric evolution during hy-dromecanical loading of a compacted silt. International Journal for Numerical and Analytical Methods in Geomechanics 28(6): 483-499

Delage, P., Audiguier, M., Cui, Y.-J. & Howat, M.D. 1996

Microstructure of compacted silt. Canadian Geotechnical Journal 33: 150-158

Delage, P. & Lefebvre, G. 1984

Study of the Structure of a Sensitive Champlain Clay and of Its Evolution During Con-solidation. Canadian Geotechnical Journal 21(1): 21-35

Geiser, F. 1999

Mechanical behaviour of an unsaturated silt – Experimental study and con-stitutive modelling (in French). PhD thesis, Lausanne, Switzerland, 224 pages

Gens, A., Alonso, E.E., Suriol, J. & Lloret, A. 1995

Effect of structure on the volumetric behavior of a compacted soil. In Alonso, E.E. & Delage, P. (eds.), Unsaturated Soils: Proceedings 1st International Conference on Unsaturated Soils / UNSAT 95: 83-88. Paris

Griffiths, F.j. & Joshi, R.C. 1990

Change in pore size distribution due to consolidation of clays. Géotechnique 40(2): 303-309

Juang, C.H. and Holtz, R.D. 1986

A probabilistic permeability model and the pore size density function, International Journal of Numerical and Analytical Methods in Geomechanics, 10, 543-553.

Koch S., and H. Flühler 1993

Non-reactive solute transport with micropore diffusion in aggregated porous media determined by a flow-interruption method. J. Contaminant Hydrology 14:39-54

Koliji, A., Laloui, L. & Vulliet L. 2004

Mathematical analysis of the hydric behaviour of structured soils, Proc. XIth Int. Symp. On Numerical Meth. In Geomechanics (NUMOG), Ottawa, pp. 31-36.

Lambe, T.W. 1958

The engineering behaviour of compacted clays. Journal of the Soil Mechanics and Foundation Division ASCE 84: 1-35

Lapierre, C., Leroueil, S. & Locat, J. 1990

Mercury intrusion and permeability of Louisville clay. Canadian Geotechnical Journal 27: 761-773

Penumadu, D. and Dean, J. 2000

Compressibility effect in evaluating the pore size distribution of kaolin clay using mercury intrusion porosimetry, Canadian Geotechnical Journal, 37, pp. 393-405.

Simms, P.H. & Yanful, E.K. 2001

Measurement and estimation of pore shrinkage and pore distribution in a clayey till during soil-water characteristic curve tests. Canadian Geotechnical Journal 38(4): 741-754

Simms, P.H. & Yanful, E.K. 2002

Predicting soil-water characteristic curves of compacted plastic soils from measured pore-size distribution. Géotechnique 52(4): 269-278

Sivakumar, V. and Wheeler, S.J., 2000

Influence of compaction procedure on the mechanical behaviour of an unsaturated compacted clay. Part 1: wetting and isotropic compression, Géotechnique, 50, pp. 359-368.

Tamari, S. 1984

Relation between pore-space and hydraulic properties in compacted beds of silty-loam aggregates. Soil Technoligy 7: 57-73

Tuncay, K. & Corapcioglu, M.Y. 1995

Effective stress principle for saturated fractured porous media. Water Resources Research 31(12): 3103-3106

Valliappan, S. & Khalili, N. 1990

Flow through fissured porous media with deformable matrix. International Journal for Neumerical Methods in Engineering 29: 1079-1094

Wang, H.F. & Berryman, J.G. 1996

On Constitutive Equations and effective stress principles for deformable, double-porosity media. Water Resources Research 32(12): 3621-3622